DESIGN AND TESTING OF A DOUBLE FAN HIGH-PRESSURE IMPURITY REMOVAL AND CLEANING DEVICE FOR FRESH CORN HARVESTERS

Xin Zhang[1], Yiwen Yuan[2], Meiling Nie[1], Zhibo Li[1], Tong Ye[1*]

[1*]Corresponding author. Heilongjiang Academy of Agricultural Machinery Engineering Sciences /Harbin, China.
E-mail: 15846594108@163.com | ORCID ID: https://orcid.org/0009-0001-8263-5178

KEYWORDS	ABSTRACT
Fresh corn, harvester, double fan, stalk crushing blade, trials	In response to the problems of high impurity content in ears and poor stalk crushing efficiency during the harvesting of fresh corn, a double fan high-pressure impurity removal and cleaning device was designed based on the operating conditions and mechanical analysis of harvester. Field trials were conducted using fan speed (1200 rpm, 1300 rpm and 1400 rpm) and harvester operating speed (6 km/h, 8 km/h and 10 km/h) as test conditions, with ear impurity content rate and stalk crushing length qualification rate as indicators. Ear impurity content rate ranged from 0.25% to 0.50% and stalk crushing length qualification rate ranged from 96.1% to 98.6%, with test results meeting operation standard under all test conditions. The designed device was able to meet the operational requirements.

HIGHLIGHTS:

For farmers growing fresh corn, it is essential to promote a harvester with a high-pressure impurity removal device.

The device is effective for both stalk crushing and impurity removal.

The provision of high-pressure impurity technology can reduce the difficulty of processing subsequent products associated with fresh corn in order to reduce costs, while at the same time speeding up the decomposition time of stalk in the field and creating good growing conditions for crop.

INTRODUCTION

Fresh corn has high nutritional value, can be eaten directly and have a good taste, and can also be subsequently processed into corn -related goods, which are popular with consumers (Li et al., 2019). Due to high economic value of fresh corn, its planting area is also expanding year by year. Fresh corn must be processed within 4 hours after harvest. If impurity content is high, it will increase the post-processing time, which will not only increase labor costs but also reduce product quality (Zhao et al., 2011). However, current level of mechanization of fresh corn ears harvesting is low. After harvest, content of impurities such as residue and leaves in the harvested ears is high, which has an impact on subsequent processing (Wang et al., 2017). Currently, fresh corn harvesters have a low length qualification rate after crushing stalks, making it difficult to rot and decompose after returning stalks to field, resulting in an increased stalk load on the tillage surface (Flower et al., 2021).

For cleaning and impurity removal devices, domestic and foreign scholars have conducted extensive research and designed devices that meet different needs. Casarsal et al. (2011) measured non-intrusive high-resolution measurements of flow field inside cross-flow fans proved that fan speed can affect impurity removal efficiency. Chu et al. (2011) carried out simulation of the cleaning device by means of coupled simulation between Fluent and EDEM software to obtain the movement pattern of threshed mixture. Craessaerts et al. (2010a) and Craessaerts et al. (2010b) established a non-linear prediction model and control method based on experimental data and fuzzy control technology suitable for use in harvesting environmental conditions with a large number of parameters for cleaning work. Zhou et al. (2020) optimized the negative pressure device of fan and designed crushing blades, which reduced impurity content of ear and improved impurity removal efficiency of the device. Liang et al. (2019) designed a dual outlet multi-channel

centrifugal fan matched to an oblique tangential combine harvester cleaning device, which can effectively stratify the mixture. Zhang et al. (2016) designed a corn harvester with a stalk cutting and conveying device, and rotor cutter was used as a stalk cutting device and worked well.

The existing harvester cleaning devices have low wind power and can meet the general cleaning requirements. However, for fresh corn harvesters, where stalk moisture content is high during operation the requirement for a lower impurity content rate on ears, higher requirements are needed for cleaning and impurity removal devices. There is relatively little research on the harvesting of fresh corn (Luo et al., 2023; Zhang et al., 2022a; Zhang et al., 2023). However, there is a lack of devices to address high impurity content and low qualified stalk length. Therefore, this paper designed a double fan high-pressure impurity removal device in order to reduce impurity content rate in the ears during the harvest of fresh

corn and improve the stalk crushing qualification rate, reduce the difficulty of subsequent processing of fresh corn in order to increase profits and speed up decomposition time of straw in the field to create good growing conditions for crop.

MATERIAL AND METHODS

Fan operation analysis and design

The high-pressure impurity removal device consists of primary and secondary double impurity removal fans, the function of which is to suck stalks from the mixture of ears and stalks cut by the cutting table and conveyed by the spiral winch into the fan, the stalks are broken up by stalk crushing blades installed coaxially with impeller of fan and thrown into field by radial wind generated by fan. The overall structure of impurity removal and cleaning device is shown in Figure 1.
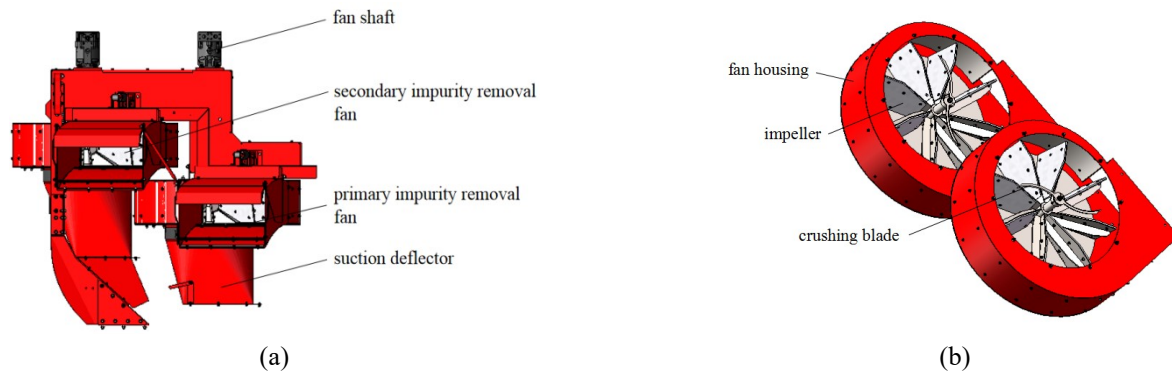

| (a) | (b) |

FIGURE 1. Structure of impurity removal and cleaning device (a) overall structure of the fan (b) simplify the internal structure of the rear fan.

In order to ensure that stalks with a large water content can be sucked into fan, the fan should have sufficient full pressure and impeller speed is an important factor affecting full pressure (Chen et al., 2022). The full pressure and rotational speed are calculated as follows:

$$
\begin{cases}
Q = 1.04q = \mu kDB \\
V_1 = \alpha v_p \\
P_d = \dfrac{\gamma V_1^{\,2}}{2g} \\
P = P_J + P_d \\
v_r = \dfrac{Q}{S} \\
P_J = \dfrac{\rho v_r^{\,2}}{2} \\
\mu = \dfrac{\pi Dn}{60}
\end{cases}
\tag{1}
$$

Where:

Q—Fan flow rate, m³/s;

q—Feeding volume, kg/s;

D—Impeller outer diameter, m;

B—Impeller width, m;

M—Impeller outer diameter linear velocity, m/s;

K—Flow coefficient, 0.5;

V_1—Average outlet wind speed, m/s;

α—Speed coefficient , 3.5;

V_p—Stem suspension speed, m/s;

P_d—Wind-powered pressure, Pa;

γ—Air volume capacity, 11.77 N/m³;

g—Gravitational acceleration, m/s²;

P—Blower full pressure, Pa;

P_J—Fan static pressure, 100Pa;

V_r—Fan inlet air speed, m/s;

S—Fan inlet cross-sectional area, m²;

ρ—Air density at standard conditions, 1.29 kg/m³,

n—Fan speed, rpm.

For a 6-row fresh corn harvester, the feed per unit time is:

$$q = \frac{6m_0V_2}{d} \qquad (2)$$

Where:

m_0—Mass of individual stalks fed to cutting table, kg;

V_2—Forward speed of harvester, m/s,

d—Plant spacing, m.

The common operating speed of the harvester is 6 km/h. The relevant data were measured on actual corn in the field, the plant spacing is 0.2 m, theoretical calculation of stalk feeding volume per unit time is 9 kg/s, single stalk mass fed into the cutting deck is 0.18 kg, the outer diameter of impeller is 860 mm. The actual measurement in the field shows that the length of main distribution section of the stalk mass fed into the cutting deck is 700 mm and average diameter is 28 mm, fan blade speed is calculated to be 1306 rpm and full pressure of fan is 820.83 Pa. Combined with dimensions of main distribution section of stalk mass fed into cutting table, wind force of fan on a single stalk is 16.1 N, which is greater than the weight of single stalk and can be sucked into fan.

The number of turbine blades is calculated according to Eck's law as (Lv et al., 2022):

$$Z = \frac{4\pi}{1.5} \frac{\sin\beta}{1 - \dfrac{D_1}{D}} \qquad (3)$$

Where:

Z—Number of blades;

β—Flow angle at blade exit, （°）,

D_1—Blade inlet diameter, m.

According to fan structure size, blade inlet diameter is taken as 80 mm, in order to facilitate the installation, the flow angle at the design blade outlet is 120°, combined with previous data can calculate the number of fan blades for 8.

In addition to the casing, the main operating components inside the impurity removal fan include fan back plate, fan blades, nylon protective plate, blade reinforcement rib, and fan shaft sleeve, with the overall structure shown in Figure. 2a.
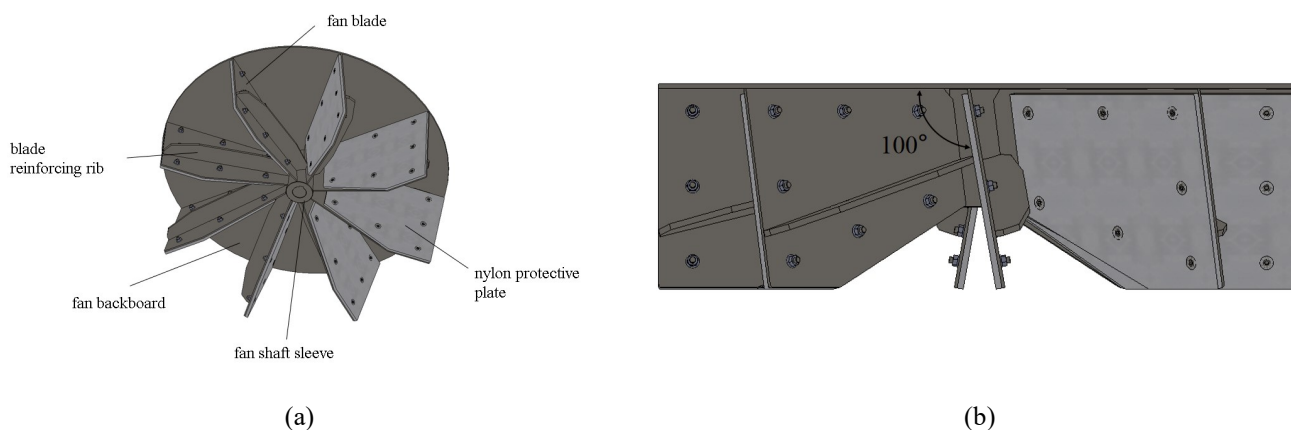

(a)

(b)

FIGURE. 2 Structural diagram of fan blade combination (a) Construction name, and (b) Blade installation angle.

The fan blades were evenly welded onto the shaft sleeve. In order to improve the safety of the fan and avoid blade breakage during high-speed rotation, nylon protective plates and blade reinforcing ribs are installed on both sides of the blades through bolts. During installation, the angle between the blade and the fan back plate was 100°, as shown in Figure. 2b.

The fan blades, fan back plate, reinforcing ribs, and nylon protective plates were shown in Figure. 3. The fan blades were connected to the fan back plate through Part a in Figure. 3a and 3b. The fan blades and reinforcing ribs were connected together through Part b in Figure. 3a and 3c, and the root of the reinforcing ribs was welded to the fan shaft sleeve. The overall dimensions of the fan blades were consistent with those of the nylon protective plates, and the external dimensions a, b, c, and d were designed to be 160mm, 340mm, 256mm, and 128mm, respectively, with a thickness of 5mm. The circular holes in Figure. 3a and 3d were bolt holes used to connect the fan blades to the nylon protective plate.
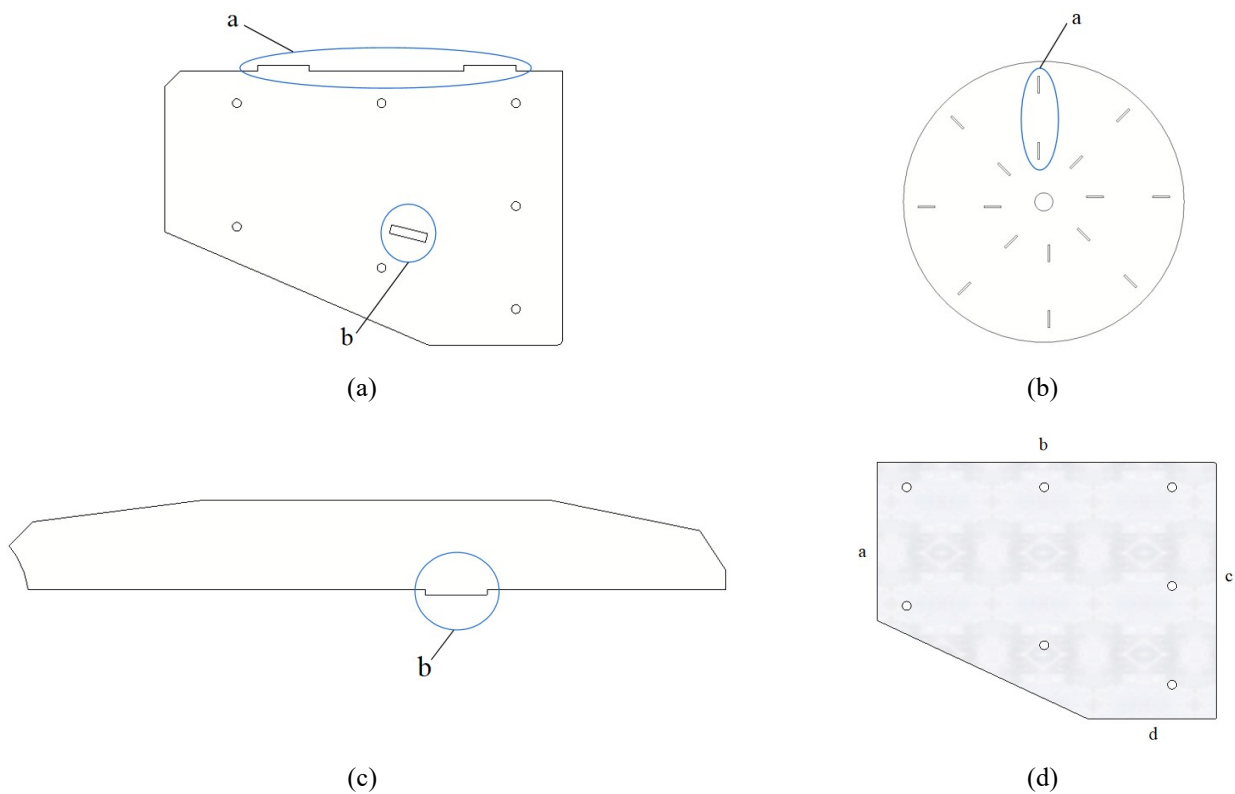
(a)

(b)

(c)

(d)

FIGURE. 3 Fan components (a) Fan blade, (b) Fan backboard, (c) Blade reinforcing rib, and (d) Nylon protective plate.

Mechanical analysis and design of stalk crushing blade

The stalk crushing blade is mounted coaxially with fan below fan and is fixed to fan shaft by a pin connection. In the crushing blade to crush stalk operation process, crushing blade to do rotary motion, stalk relative to crushing blade has a tendency to move outward, and because of fresh corn harvest stalk moisture content and harvester feed are large, the fan room stalk interaction, will produce stalk first contact with crushing blade cannot be directly stalk breaking, so the stalk the blade to the periphery of movement, resulting in poor stalk crushing effect of problem, in order to reduce this probability, a mechanical analysis of crushing blade's process of crushing the stalks was carried out to design a reasonable crushing blade structure, shown in Figure. 4.
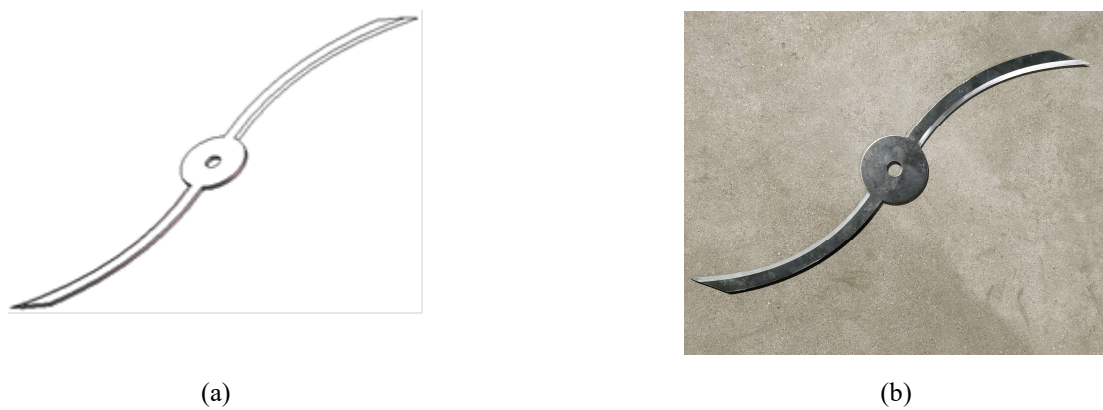

(a)

(b)

FIGURE 4. Stalk crushing blade (a) schematic diagram of the structure, (b) physical image.

For theoretical analysis, shown as Figure. 5, stalk is considered as a mass point, crushing blade rotates at constant speed, and interaction between stalk and crushing blade is ignored. With stalk section A as the coordinate origin, crushing blade inner edge surface tangential direction for X-axis, the normal direction for Y-axis to establish a plane coordinate system. θ is the angle between normal relative acceleration of stalk and Y-axis, φ is the angle between stalk implication acceleration and negative half axis of X-axis.
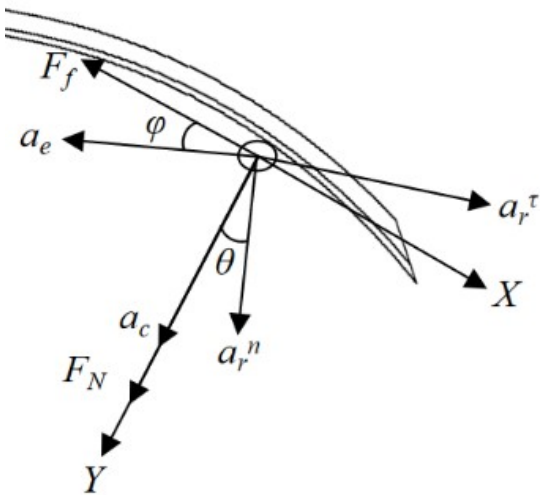
Note: F_f is tangential friction of crushing blade edge against stalk, m/s; a_e= is stalk implicated acceleration, m/s^2; a_c is stalk Coriolis acceleration, m/s^2; F_N is stalk striking force by crushing blade, N; a_r^n is normal acceleration of the stalk relative to crushing blade, m/s^2; a_r^τ is stalk tangential acceleration relative to crushing blade, m^2/s.

FIGURE 5. Analysis of pulverizing blade crushing stalks.

The interaction between crushing blade and the stalk is analyzed and mechanical equations for stalk mass:

$$\begin{cases} m\left(a_r^\tau \cos\theta + a_r^n \sin\theta - a_e\cos\varphi\right) - F_f = ma_x \\ m\left(a_e\sin\varphi + a_c + a_r^n\cos\theta\right) + F_N = ma_y \\ a^2 = a_x^2 + a_y^2 \\ F_f = \mu_1 ma_x \\ a_e = \omega^2 r \\ a_c = 2\omega\dfrac{dl}{dt} \\ a_r^n = \dfrac{\left(\dfrac{dl}{dt}\right)^2}{\rho_A} \\ a_r^\tau = \dfrac{d^2l}{dt^2}\rho_A \\ l = r\cos\varphi \end{cases} \qquad (4)$$

Where:

M—Stalk quality, kg;

a_x—Stalk acceleration in X-axis direction, m^2/s;

a_y—Stalk acceleration in the Y-axis direction, m^2/s;

a—Stalk acceleration, m^2/s;

μ_1—Friction between the crushing blade edge and the stalk, N;

ω—Angular speed of crushing blade rotation, rpm;

r—Stalk radius of rotation, m;

l—Projection of radius of rotation of stalk on the tangent of blade, m;

t—Time, s,

ρ_A—Curvature radius of stalk at cutting edge, m.

By organizing [eq. (4)], we can obtain:

$$a = \sqrt{\left\{\frac{\dfrac{F_N}{m} + \omega^2 r\sin\varphi + \dfrac{2\omega d(r\cos\varphi)}{dt} + \dfrac{\left[\dfrac{d(r\cos\varphi)}{dt}\right]^2\cos\theta}{\rho_A}}{}\right\}^2 + \left\{\frac{\dfrac{d^2(r\cos\varphi)}{dt^2}\rho_A\cos\theta + \dfrac{\left[\dfrac{d(r\cos\varphi)}{dt}\right]^2}{\rho_A}\sin\theta - \omega^2 r\cos\varphi}{1+\mu_1}\right\}^2} \qquad (5)$$

From [eq. (5)], it can be seen that movement of stalk is influenced by rotation angle speed, rotation radius, and friction coefficient of crushing blade. The greater speed and rotation radius, the more pronounced the tendency for stalk to move towards outer circle of crushing blade, resulting in a high intensity of work for outer circle of crushing blade and a low intensity of work for inner circle, reducing overall operational efficiency. Therefore, crushing blade shape is designed as a hyperbolic spiral to improve efficiency of crushing blade.

The hyperbolic solenoid parametric equation is

$$\begin{cases} x = \dfrac{b\cos\psi}{\psi} \\ y = \dfrac{b\sin\psi}{\psi} \end{cases} \qquad (6)$$

Where:

b—Horizontal asymptote coordinates,

ψ—The angle between any point on the line and the line of origin，(°)

The curvature at any point on the curve is

$$\left(\frac{\frac{dy}{d\psi}}{\frac{dx}{d\psi}}\right) = \frac{\sin\psi - \psi\cos\psi}{\psi\sin\psi + \cos\psi} \tag{7}$$

Derivative of curvature at any point:

$$\left(\frac{\sin\psi - \psi\cos\psi}{\psi\sin\psi + \cos\psi}\right)' = \frac{\psi^2}{(\psi\sin\psi + \cos\psi)^2} \tag{8}$$

From the above equation, the hyperbolic spiral is monotonically increasing from F to E. This in turn leads to:

$$y = \sqrt{\frac{b^2}{\psi^2} - x^2} \tag{9}$$

We set the coordinates of E and F as (x_1, y_1), (x_2, y_2), respectively, and the intersection of the two points on the plane as G, shown as Figure 6.

$$\begin{cases} l_{FG} = x_2 - x_1 \\ l_{EG} = y_2 - y_1 \\ l_{EF}^2 = l_{EG}^2 + l_{FG}^2 \end{cases} \tag{10}$$
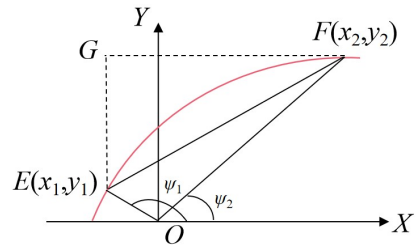
Combining eqs (9) and (10), we can obtain:

FIGURE 6. Hyperbolic spiral.

$$l_{EF}^2 = \frac{b^2}{\psi_2^2} + \frac{b^2}{\psi_1^2} - \frac{b^2}{\psi_1\psi_2}(\sin\psi_1\sin\psi_2 + \cos\psi_1\cos\psi_2) \tag{11}$$

From Formula (11) can be seen, curve shape by ψ_1, ψ_2 and l_{EF} three parameters to determine, where l_{EF} is known to be 0.39 m. In order to convenience of subsequent workpiece processing, ψ_1 and ψ_2 are taken as 90 °and 45 °. The parameter b is calculated by Formula (11) to be equal to 23.8. Therefore, the parameter equation of hyperbolic spiral is finally determined as:

$$\begin{cases} x = \frac{23.8\cos\psi}{\psi} \\ y = \frac{23.8\sin\psi}{\psi} \end{cases} \tag{12}$$

The physical object of the dual fan high-pressure impurity removal device obtained through processing is shown in Figure 7.
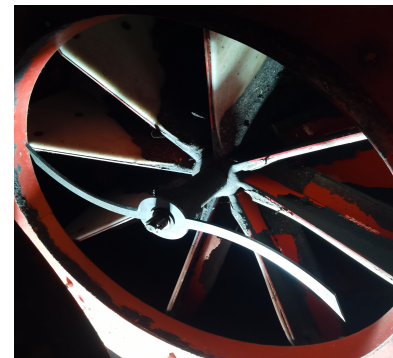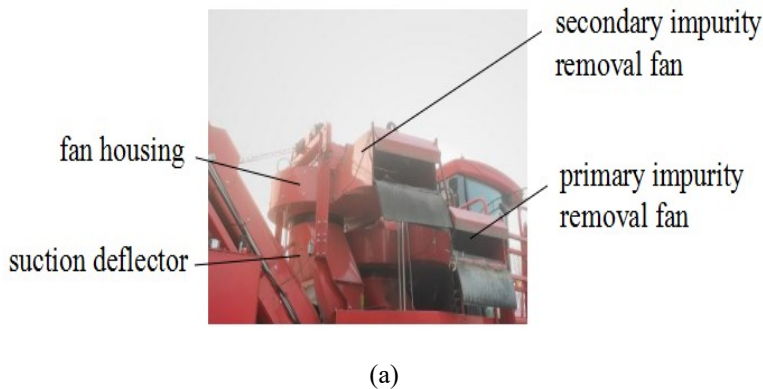

FIGURE 7. Physical drawing of double fan high-pressure impurity removal and cleaning device (a) whole view, (b) bottom view of impurity removal fan interior after removing the casing.

Field experiment

In order to verify rationality of design, field validation trials were conducted on a double fan high pressure impurity removal and cleaning device. The trial was carried out in August 2022 on a farm in Keshan County, Heilongjiang Province (E125°10′57″-126°8′18″, N47°50′51″-48°33′47″) on flat terrain with a continental climate and typical black loam soil, with a monopoly spacing of 650 mm and a plant spacing of 200 mm. The harvester cut the stubble to a height of 100 mm. The average total weight of a single plant is 330.5 g, and the average weight of fruit ears accounts for 84.8%. And the average length of an ear is 195.6 mm.

The moisture content of fresh corm stalk is large and has a major impact on the effectiveness of harvester, so stalk moisture content was measured. Randomly select 5 plots of land and measure the moisture content of 5 stalks per plot, and calculate average moisture content of each plot of stalk, shown as Figure 8.

FIGURE 8. Sampling of stalk.

According to GB/T 1927.4-2021, the moisture content of stalk (w.b) was calculated as:

$$\omega_1 = \frac{m_1 - m_2}{m_1} \times 100\% \qquad (13)$$

Where:

ω_1—Moisture content, %;

m_1—Total material mass before drying, g,

m_2—Total material mass after drying, g

The average moisture content (w.b) of measured each group of stalk was calculated to be $82.15 \pm 1\%$.

The forward speed and fan speed will affect the operation effect of the fresh corn harvester (Kang et al., 2019; Zhou et al., 2019). In order to optimize the operation parameters of the device, the fan rational speed and forward speed were selected as the test factors, and the orthogonal design of experiments was used to optimize the parameters. Each group of tests was repeated 5 times. Commonly used harvesting parameters were selected in the experiment, with harvest rows value of 6 and corn stubble height of 100mm. The 4YX-6 fresh corn combine harvester can adjust the fan rational speed through electrical equipment, with a controllable value of 1200, 1300 and 1400 rpm; According to Zhou et al. (2020), the forward speed of the fresh corn harvester during normal operation is 6, 8 and 10 km/s, and the experimental factor codes are shown in Table 1. These two experimental factors are controlled by the electric control system of the combine harvester itself. Figures 9a and 9b show the display screens for adjusting the front fan speed (the same as the rear fan) and forward speed. Before each group of experiments, adjust the fan rotational speed and forward speed, respectively, to the desired value by adjusting the knob in Figure 9c. Before implementation, several testing areas were divided into different fields of the base, and the interarea distance was set as 10 m (measured manually using a meter ruler) (Zhang et al., 2022b). The ear impurity content rate and stalk crushing length qualification rate were used as indicators and field test process is shown in Figure 10.

(a)	(b)	(c)

FIGURE 9. Regulation of experimental factors (a) fan rotational speed setting interface, (b) forward speed setting interface, and (c) control deck.

TABLE 1 Test factors and levels.

Level	Factors	
	Fan rotational speed A (rpm)	Forward speed B (km/h)
1	1200	6
2	1300	8
3	1400	10

FIGURE 10. Field experiment.

Two experimental indicators were measured as suggested by Zhou et al (2020). Collect the material after fan operation and measure the mass of impurities in material and the total mass of material, the ratio of the two is ear impurity content rate, calculated as:

$$G_n = \frac{W_n}{W_P} \times 100\% \qquad (14)$$

Where:

G_n—Ear impurity content rate, %;

W_n—Impurity mass, g,

W_P—Total mass of material after fan operation, g.

Collect the stalks discharged through discharge deflector and randomly select 5 test samples of 1 m² after each harvester operation, where stalks greater than 50 mm in length (measured by 200mm steel ruler) are unqualified stalks, measure their total mass and then measure the total mass by electronic balance of discharged impurities, stalk crushing length qualification rate is calculated as:

$$\eta = \left(1 - \frac{m_3}{M}\right) \times 100\% \qquad (15)$$

Where:

η—Passing rate, %;

m_3—Unqualified stalk mass, g,

M—Total mass of discharged impurities, g.

RESULTS AND DISCUSSION

The trail results of ear impurity content rate are shown in Table 2.

TABLE 2. Ear impurity content rate.

Rotation speed/（rpm）	Impurity content rates at different speeds/%		
	6	8	10
1200	0.36	0.38	0.48
	0.33	0.36	0.46
	0.33	0.40	0.43
	0.38	0.41	0.45
	0.32	0.35	0.50
1300	0.32	0.34	0.45
	0.33	0.36	0.42
	0.31	0.32	0.39
	0.30	0.40	0.47
	0.31	0.38	0.48
1400	0.29	0.32	0.37
	0.28	0.31	0.35
	0.29	0.32	0.32
	0.25	0.29	0.37
	0.26	0.27	0.31

The data of impurity rate was conducted analyzed by variance, and shown in Table 3. It can be observed that p<0.0001 of the model, indicating that the regression equation is significant and can be describe the relationship between each factor, except cross term AB, and response value. After excluding insignificant factors, we obtained the regression mathematical model of ear impurity content rate Y_1:

$$Y_1 = 0.727 - 0.000447A + 0.026B \tag{16}$$

TABLE 3. Variance analysis of the ear impurity content.

Source	Sum of Squares	df	Mean Squares	F-Value	p-Value
Cor Model	.156	8	.020	28.910	1.88E-13**
A	.064	2	.032	47.383	8.25E-11**
B	.087	2	.043	64.240	1.33E-12**
AB	.005	4	.001	2.008	.114
Error	.024	36	.001		
Total	5.955	45			
Cor Total	.181	44			

Note: ** means highly significant (p<0.01), and * means significant (0.01≤P<0.05).

When forward speed of harvester was 6km/h and fan speed was 1200, 1300 and 1400 rpm, average ear impurity content rate was 0.34%, 0.31% and 0.27%, respectively; When forward speed of harvester was 8km/h and fan speed was 1200, 1300 and 1400 rpm, average impurity content rate in ears was 0.38%, 0.36% and 0.30%, respectively. At a harvester speed of 10 km/h and fan speeds of 1200, 1300 and 1400 rpm, average ear impurity content rate was 0.46%, 0.44% and 0.34% respectively, with a range of 0.25% to 0.50%. Compared with the 0.71% impurity content rate in ears of cleaning device of Zhou et al. (2020), overall impurity content rate was lower than 0.71%, with the maximum impurity content rate of the designed cleaning device in this paper being 29.5% lower and the minimum impurity content rate 64.8% lower.

Similarly, the impurity content rate of the negative pressure impurity removal device for fresh corn harvesting was 1.31% lower than that optimized by Zhou et al. (2023). When forward speed was certain, with increase of the fan speed, impurity content rate gradually decreased and cleaning effect gradually increased. This is because fan speed increased, wind force increased and cleaning effect is better. When fan speed was certain and forward speed increased, impurity content rate gradually increased and cleaning effect gradually decreased. This is because forward speed becomes larger, feeding volume increased and wind force generated by fan is not sufficient to fully discharge stalk from fan, resulting in a poor cleaning effect.

The trail results of stalk crushing length qualification rate are shown in Table 4

TABLE 4. Stalk crushing length qualification rate.

Rotation speed/（rpm）	Qualification rates at different speeds/%		
	6	8	10
1200	97.1	96.8	96.2
	96.8	96.8	96.7
	96.7	96.9	96.2
	97.0	96.6	96.3
	96.9	97.1	96.1
1300	97.3	97.2	96.9
	97.0	96.8	96.3
	97.2	97.1	97.0
	96.9	96.3	97.1
	97.2	97.4	97.0
1400	98.1	98.0	97.6
	98.3	98.1	97.8
	98.6	97.9	97.6
	98.6	97.9	97.4
	98.2	97.7	98.0

Similarly, we used SPSS 23.0 software to conduct variance analysis for Table 4; the results are given in Table 5.

TABLE 5. Variance analysis of stalk crushing length qualification rate.

Source	Sum of Squares	df	Mean Squares	F-Value	p-Value
Cor Model	16.507	8	2.063	33.581	1.88E-14[**]
A	14.054	2	7.027	114.362	2.53E-16[**]
B	1.990	2	.995	16.192	1E-5[**]
AB	.464	4	.116	1.886	.134
Error	2.212	36	.061		
Total	425307.61	45			
Cor Total	18.719	44			

Note: [**] means highly significant (p<0.01), and [*] means significant (0.01≤P<0.05).

Table 5 shows that the stalk crushing length qualification rate regression model's significance test value (p<0.01) demonstrates that the qualification rate regression model extremely significant. Except for the cross item AB, which is insignificant, the qualification rate regression model is significant. The significance of the influence of each variable on the qualification rate is in the following order, from more to less significant: fan rotational speed and travel speed. After eliminating the non-significant factors, the regression equation of each variable on stalk crushing length qualification rate was obtained, as shown in [eq. (17)]:

$$Y_2 = 89.749 + 0.007A - 0.128B \qquad (17)$$

When forward speed of the harvester was 6 km/h and fan speed was 1200, 1300 and 1400 rpm, stalk crushing length qualification rate was 96.9%, 97.1% and 98.3% respectively; When forward speed of harvester was 8 km/h and fan speed is 1200, 1300 and 1400 rpm, stalk crushing length qualification rate was 96.8%, 97.0% and 97.9%, respectively. When harvester advanced at a speed of 10km/h and fan speeds were 1200, 1300, and 1400 rpm,

respectively, qualified rates were 96.3%, 96.7%, and 97.7%, respectively. Overall, this device has an average stalk crushing length qualification rate of 96.1% to 98.6%. Compared with the experimental results, it was generally higher than 96.2% measured by Zhou et al. (2020), among which the minimum qualification rate of the designed impurity removal and cleaning device was 0.01% lower than it, and the maximum qualification rate was 0.25% higher than it. Similarly, stalk crushing length qualification rate for the stalks and leaves cleaning device of the fresh corn ear harvester designed by Zhou et al. (2019) is 88.59~89.27%. When forward speed was constant, as fan speed increased, qualified rate gradually increased, and stalk crushing effect gradually improved. This is because as fan speed increases, the probability of stalk crushing blade contacting stalk increases, and crashing effect improves. When fan speed was constant and forward speed increased, stalk crushing length qualification rate gradually decreased, and stalk crushing effect gradually decreased. This is because forward speed increases, feeding amount increases, and speed of crushing blade is not enough to completely cut the stalk discharged by cleaning unit, resulting in poor straw crushing effect.

CONCLUSIONS

1. In this paper, a double fan high-pressure impurity removal and cleaning device was designed, taking into account the operating conditions of fresh corn harvester and mechanical analysis between stalk and crushing blade. The main parameters such as fan speed, full pressure, number of blades and crushing blade structure were determined.

2. The designed device was tested in the field with fan speed (1200 rpm, 1300 rpm, 1400 rpm) and harvester operating speed (6 km/h, 8 km/h, 10 km/h) as test conditions, and ear impurity content rate and stalk crushing length qualification rate as indicators.

3. During the trials, ear impurity content rate ranged from 0.25% to 0.50% and stalk crushing length qualification rate ranged from 96.1% to 98.6% under different operating conditions. The results under all test conditions met the standards and the designed device was able to meet the operational requirements.

REFERENCES

Casarsa L, Giannattasio P (2011) Experimental study of the three-dimensional flow field in cross-flow fans. Experimental Thermal and Fluid Science 35(6): 948-959. https://doi.org/10.1016/j.expthermflusci.2011.01.015

Chen N., Tian LQ, Zhang ZZ, Li L, Wang ZM, Chen DJ (2022) Design and experiment on double conical centrifugal cleaning fan of head-feed combine harvester. Transactions of the Chinese Society for Agricultural Machinery 53(12): 193-202. https://doi.org/10.6041/j.issn.1000-1298.2022.12.018

Chu KW, Wang B, Xu DL, Chen YX, Yu AB (2011) CFD-DEM simulation of the gas-solid flow in a cyclone separator. Chemical Engineering Science 66(5): 834-847. https://doi.org/10.1016/j.ces.2010.11.026

Craessaerts G, Baerdemaeker JD, Missotten B, Saeys W (2010a) Fuzzy control of the cleaning process on a combine harvester. Biosystems Engineering. 106(2): 102-111. https://doi.org/10.1016/j.biosystemseng.2009.12.012

Craessaerts G, Saeys W, Missotten B, Baerdemaeker JD (2010b) Identification of the cleaning process on combine harvesters, Part II: a fuzzy model for prediction of the sieve losses. Biosystems Engineering 106(2): 97-102. https://doi.org/10.1016/j.biosystemseng.2009.11.009

Flower KC, Ward PR, Micin SF, Cordingley N (2021) Crop rotation can be used to manipulate residue levels under no-tillage in a rainfed Mediterranean-type environment. Soil and Tillage Research 212: 105062. https://doi.org/10.1016/j.still.2021.105062

Kang NR, Choi I S, Kim YK, Choi Y, Yu SH, Woo JK, Hyun CS, Kim SK (2019) Performance evaluation and design of an edible fresh corn harvesting machine. Journal of drive and control 16(4): 74–79. https://doi.org/10.7839/ksfc.2019.16.4.074

Li TY, Zhou FJ, Guan XD, Wu H (2019) Design and experiment on flexible low-loss fresh maize picking device. International Agricultural Engineering Journal 28(2): 233-247.

Liang ZW, Li YM, Baerdemaeker JD, Xu LZ, Saeys W (2019) Development and testing of a multi-duct cleaning device for tangential-longitudinal flow rice combine harvesters. Biosystems Engineering 182: 95-106. https://doi.org/10.1016/j.biosystemseng.2019.04.004

Luo H, Nie J, Zhang L (2023) Design and test of a dislocation baffle roller bionic picking device for fresh corn. Agriculture 13(5): 991. https://doi.org/10.3390/agriculture13050991

Lv JQ, Zhu MF, Zhu XX, Li JH, Su WH, Liu ZY (2022) Optimal design and experiment of integrated fan of air suction potato planter. Transactions of the Chinese Society for Agricultural Machinery 53(3): 80-90. https://doi.org/10.6041/j.issn.1000-1298.2022.03.008

Wang XR, Geng LX, Li XP, Pang J, Zhou HP (2017) Design and experiment of low-injury picking test table for fresh-eating maize. Agricultural Engineering 7(1): 68-71.

Zhang H, Chen B, Li Z, Zhu C, Jin E, Qu Z (2022a) Design and simulation analysis of a reverse flexible harvesting device for fresh corn. Agriculture 12(11): 1953. https://doi.org/10.3390/agriculture12111953

Zhang L, Yu J, Zhang Q, Liu C, Fang X (2023) Design and experimental study of bionic reverse picking header for fresh corn. Agriculture 13(1): 93. https://doi.org/10.3390/agriculture13010093

Zhang YP, Diao PS, Du RC, Liu LL, Zhang J (2016) Design and test of stalk chopping and conveying device for maize combine reaping both stalk and spike. Transactions of the Chinese Society for Agricultural Machinery 47(s1): 208-214. https://doi.org/10.6041/j.issn.1000-1298.2016.S0.032

Zhang YW, Yin YX, Meng ZJ, Chen D, Qin WC, Wang Q, Dai D (2022b) Development and testing of a grain combine harvester throughput monitoring system. Computers and Electronics in Agriculture 200: 107253. https://doi.org/10.1016/j.compag.2022.107253

Zhao YQ, He XP, Shi JF, Liu Q, Shao G, Xie QZ (2011) Design and experiment of sweet and waxy corn husker. Transactions of the Chinese Society of Agricultural Engineering 27(2): 114-118.

Zhou FJ, Guan XD, Tang ZF, Wu H (2020) Parameter optimization and experiment of negative pressure impurity removal device for fresh maize ear harvest. Transactions of the Chinese Society for Agricultural Machinery 51(11): 138-147.

Zhou FJ, Wei Y, Wu H, Zhang MH (2019) Design of stalks and leaves cleaning device for fresh maize ear harvester Journal of Northeast Agricultural University 50(4):79-87. https://doi.org/10.19720/j.cnki.issn.1005-9369.2019.4.0010

Zhou FJ, You K, Li TY, Guan XD (2023) Parameter optimization of negative pressure impurity removal and secondary stem pulling device for fresh corn harvest. Journal of Northeast Agricultural University 54(3): 71-82. https://doi.org/10.19720/j.cnki.issn.1005-9369.2023.03.0